CHEMISTRY
A EUROPEAN JOURNAL

DOI: 10.1002/chem.200501077

One-Electron Redox Processes during Polyoxometalate-Mediated Photocatalytic Reactions of TiO_2 Studied by Two-Color Two-Laser Flash Photolysis

Takashi Tachikawa, Sachiko Tojo, Mamoru Fujitsuka, and Tetsuro Majima*[a]

Abstract: The one-electron redox processes of several compounds during polyoxometalate (POM)-mediated photocatalytic reactions of TiO_2 were investigated using the two-color two-laser flash-photolysis technique. The efficiency of the one-electron oxidation of aromatic sulfides by the trapped hole (h_{tr}^+) or the surface-bound OH radical ($OH_s^\bullet$) is found to be significantly enhanced due to electron transfer from the conduction band (CB) of TiO_2 to the POM. The efficiency of the electron transfer from the CB of TiO_2 to the POM decreases in the order $H_2W_{12}O_{40}^{6-} < SiW_{12}O_{40}^{4-} < PW_{12}O_{40}^{3-}$, that is, it depends on the reduction potential (E_{red}) of the POMs. Electron injection from $PW_{12}O_{40}^{4-}$ in the excited state ($PW_{12}O_{40}^{4-*}$) to the CB of TiO_2 was clearly observed using the two-color two-laser flash-photolysis technique. Storage of electrons in the $TiO_2/PW_{12}O_{40}^{3-}$/methyl viologen (MV^{2+}) ternary system was also achieved upon two-color two-laser irradiation.

Keywords: electron transfer · photochemistry · polyoxometalates · radical ions · titanium oxide

Introduction

Semiconductor-based nanocomposite materials are expected to have a significant impact on the fields of optoelectronics, catalysis, and biochemistry.[1] To date, many attempts have been made to improve the photocatalytic ability of TiO_2 nanoparticles with various metals and ions because TiO_2 has been extensively used in areas such as environmental purification, hydrogen production, gas sensors, and dye-sensitized solar cells.[2] Typically, the reaction processes are initiated by the band-gap excitation of the TiO_2 particles with UV irradiation to generate reactive species, such as photogenerated electrons (e^-) and holes (h^+),[3–10] $O_2^{\bullet-}$,[11] H_2O_2,[12] and OH radicals ($OH^\bullet$).[13–18] For example, it has been proposed that the surface hydroxy groups react with the holes to form surface-bound $OH^\bullet$ ($OH_s^\bullet$), which then oxidize the surface adsorbates.[2b] Recently, Nakato et al. have investigated the photooxidation of water adsorbed on the TiO_2 surface by in situ FT-IR absorption and photoluminescence methods; they concluded that the photoevolution of oxygen is initiated by nucleophilic attack of an H_2O molecule at a photogenerated h^+ at a surface lattice O site rather than by oxidation of a surface OH group by h^+.[19]

The reactivity and lifetime of these oxidizing species are thought to play an important role in controlling the overall kinetics of the oxidative processes, although the photocatalytic efficiency of TiO_2 also depends upon the degree of charge separation of the photogenerated e^- and h^+ pairs at the surface of the TiO_2 particles. To enhance the charge separation, suitable metals have been deposited on the surface of TiO_2.[20–22] However, the deposition of metal islands can be problematic because the island size can potentially grow large enough to cover the active sites.

Recently, Keggin-type polyoxometalates (POMs)[23] have been applied to TiO_2 photocatalytic systems as electron scavengers to retard the fast charge-recombination with h^+ in TiO_2 and, consequently, enhance the photocatalytic redox processes.[24–29] In addition, the POM^-, which is generated by a one-electron reduction reaction with a conduction band e^- (e_{CB}^-) in TiO_2, subsequently absorbs visible light to form the excited-state POM^- (POM^{-*}), which synergistically catalyzes the reduction of methyl orange during TiO_2 photocatalytic reactions.[24] Such an electron-transfer mechanism is analogous to the "Z-scheme" mechanism for plant photosynthetic systems. This novel nanocomposite system containing TiO_2 and a POM has the potential for application in electronic devices and medical chemistry as well as the photocatalytic degradation of organic pollutants. Therefore, a

[a] Dr. T. Tachikawa, S. Tojo, Prof. Dr. M. Fujitsuka, Prof. Dr. T. Majima
The Institute of Scientific and Industrial Research (SANKEN)
Osaka University, Mihogaoka 8–1, Ibaraki, Osaka 567-0047 (Japan)
Fax: (+81) 6-6879-8496
E-mail: majima@sanken.osaka-u.ac.jp

further understanding of the interfacial redox reactions between TiO_2 and POM and the subsequent reactions with organic molecules at the interface are very important.

Here we investigate the one-electron redox reactions that take place during POM-mediated TiO_2 photocatalytic reactions using a two-color two-laser flash-photolysis technique. This technique is a powerful tool for the investigation of electron-transfer reactions in the excited state,[30] an we have successfully applied it for understanding the mechanism of photocatalytic redox reactions. To the best of our knowledge, there is only one report concerning the investigation of TiO_2 photocatalytic reactions by two-color two-laser flash photolysis.[7a] First, we studied the influence of the POM on the photocatalytic one-electron oxidation reactions of substrates (S), such as aromatic sulfides, using a one-laser flash-photolysis technique. The one-electron oxidation processes of aromatic sulfides in a TiO_2 colloidal solution or adsorbed on a TiO_2 surface were examined. Next, we investigated the reaction dynamics of $PW_{12}O_{40}^{4-}$ in the excited state ($PW_{12}O_{40}^{4-*}$) using a two-color two-laser flash-photolysis technique. These techniques not only verify the applicability of this nanocomposite material, but also provide important information about the mechanisms of the TiO_2 photocatalytic redox reactions.

Results and Discussion

Electron transfer from the conduction band of TiO_2 to POMs: First, to clarify the electron-transfer process from the CB of the TiO_2 to the POM, we observed the transient absorption spectra during laser flash photolysis (at 355 nm) of argon-saturated TiO_2/POM colloidal solutions in which the TiO_2 nanoparticles are selectively excited by the laser pulse because of the lower absorbance of the POMs (Figure 1). All POM reactions were carried out at pH 1 because of the excellent stability of $PW_{12}O_{40}^{3-}$ at this pH.

Figure 2 shows the transient absorption spectra observed after laser irradiation at 355 nm (20 mJ per pulse) of TiO_2 and TiO_2/POM colloidal solutions at room temperature. The spectral shape is very complex because of contributions

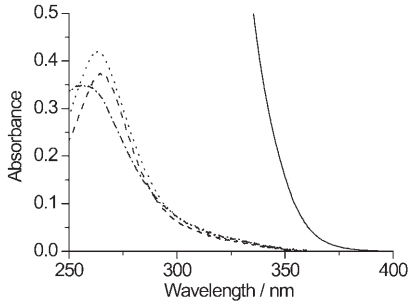

Figure 1. Steady-state UV absorption spectra observed for $H_3PW_{12}O_{40}$ (dotted line), $Na_4SiW_{12}O_{40}$ (broken line), and $(NH_4)_6H_2W_{12}O_{40}$ (dashed-and-dotted line) (0.05 mM) in acidic water (pH 1) in the absence of TiO_2 nanoparticles. The absorption spectrum of the TiO_2 colloidal aqueous solution is shown as a solid line. The optical path length is 1 mm.

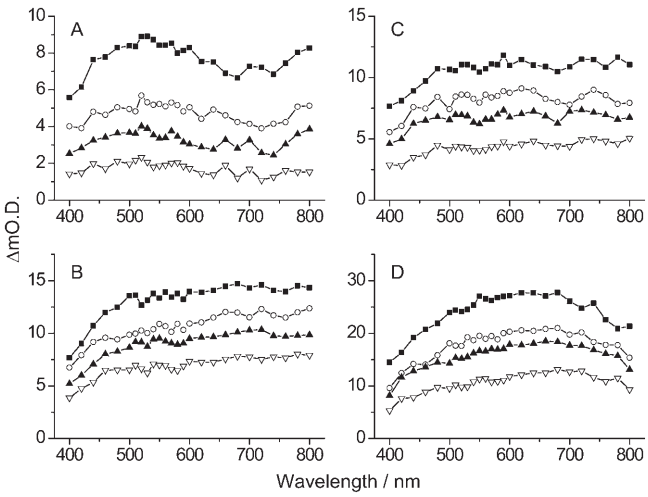

Figure 2. Transient absorption spectra observed at 0.1 (solid squares), 0.5 (open circles), 1 (solid triangles), and 5 μs (open inverted triangles) after the laser flash during the 355-nm laser photolysis of argon-saturated TiO_2 (A), $TiO_2/PW_{12}O_{40}^{3-}$ (B), $TiO_2/SiW_{12}O_{40}^{4-}$ (C), and $TiO_2/H_2W_{12}O_{40}^{6-}$ (D) colloidal solutions. The POM concentration ([POM]) is 0.05 mM.

from the trapped h^+ (h_{tr}^+) and e^- (e_{tr}^-), and POM^- in the present time and spectral ranges.[7,31,32] However, the intensities of the absorption bands observed at 0.1 μs for TiO_2/POM (Figure 2B–D) are significantly greater than that observed for TiO_2 alone (Figure 2A), and depend on the POM concentration, as shown in Figure 3. Therefore, electron transfer from the photogenerated e_{CB}^- and/or e_{tr}^- to POM occurs as given by Equations (1), (2), and (3):

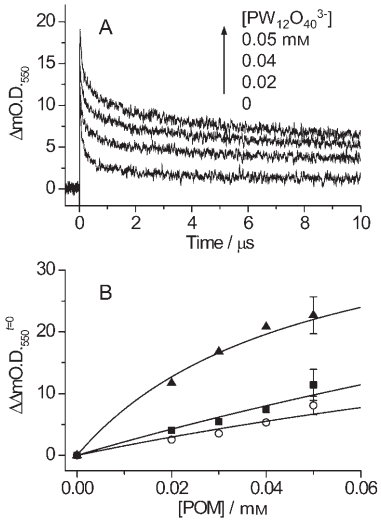

Figure 3. A) Time traces observed at 550 nm during the 355-nm laser flash photolysis of argon-saturated $TiO_2/PW_{12}O_{40}^{3-}$ (0–0.05 mM) colloidal solutions. B) Dependence of increases in the initial ΔO.D. values ($\Delta\Delta O.D.^{t=0}$) observed at 550 nm, which are calculated by subtracting the ΔO.D. value in the absence of POM from those in the presence of $PW_{12}O_{40}^{3-}$ (solid squares), $SiW_{12}O_{40}^{4-}$ (open circles), and $H_2W_{12}O_{40}^{6-}$ (solid triangles), on the POM concentration. Solid lines are visual guides.

$$TiO_2 + h\nu \rightarrow h_{VB}^{+} + e_{CB}^{-} \quad (1)$$

$$h_{VB}^{+} \rightarrow h_{tr}^{+},\ e_{CB}^{-} \rightarrow e_{tr}^{-} \quad (2)$$

$$e_{CB}^{-}(e_{tr}^{-}) + POM \rightarrow POM^{-} \quad (3)$$

The absence of the expected increase (see Figure 3A) shows that the electron transfer is completed within the laser duration of 5 ns. The transferred e^- ("blue" electron), which is located in a predominantly nonbonding b_2 orbital of the C_{4v} distorted WO_6 octahedron, is delocalized over all 12 tungsten atoms (the rate of intramolecular electron transfer is about 10^{11} to $10^{12}\,s^{-1}$ at room temperature) by a thermal hopping mechanism.[33]

Figure 3B shows the dependence of increases in the initial ΔO.D. values ($\Delta\Delta O.D.^{t=0}$) observed at 550 nm, which are calculated by subtracting the ΔO.D. value in the absence of POM from that in the presence of POM, on the POM concentration.

It was found that the apparent generation yields of POM^- increase in the order $SiW_{12}O_{40}^{4-} < PW_{12}O_{40}^{3-} < H_2W_{12}O_{40}^{6-}$. The reduction potentials (E_{red}) of $PW_{12}O_{40}^{3-}$, $SiW_{12}O_{40}^{4-}$, and $H_2W_{12}O_{40}^{6-}$ are +0.218, +0.054, and −0.162 V versus NHE,[23b] respectively, as summarized in Table 1. These values are lower than that (−0.19 V versus NHE) of e_{CB}^- at pH 1,[34] thus suggesting that the electron transfer from the CB of TiO_2 to the POM is an exothermic process.

Table 1. Reduction potential (E_{red}) of POMs, adsorption constant (K_{ad}), the ΔO.D. values assigned to POM^- ($\Delta\Delta O.D._{red}^{t=0}$), and concentration of the generated POM^- ($[POM^-]$) observed during the 355-nm laser flash photolysis of argon-saturated TiO_2/POMs colloidal solutions.

POM	E_{red}[a] [V vs. NHE]	K_{ad}[b] [$10^4\,M^{-1}$]	$\Delta\Delta O.D._{red}^{t=0}$[c]	$[POM^-]$[d] [$10^{-6}\,M$]
$PW_{12}O_{40}^{3-}$	+0.218	5.7±0.6 (1.0)[e]	0.009[f]	4.5 (1.0)[e]
$SiW_{12}O_{40}^{4-}$	+0.054	6.0±0.8 (1.1)[e]	0.006[g]	2.9 (0.6)[e]
$H_2W_{12}O_{40}^{6-}$	−0.162	20±4 (3.5)[e]	0.024[h]	11 (2.4)[e]

[a] From reference [23b]. [b] Equilibrium constants of adsorption of POMs on the P25 TiO_2 powder in water (pH 1). [c] $\Delta\Delta O.D._{red} = \Delta O.D.(TiO_2/POM) - \Delta O.D.(TiO_2)$. [d] Calculated from $\Delta\Delta O.D._{red}/\varepsilon_{red}$. [e] Relative values. [f] At 751 nm ($\varepsilon_{red} = 2000\,M^{-1}cm^{-1}$). [g] At 729 nm ($\varepsilon_{red} = 2100\,M^{-1}cm^{-1}$). [h] At 689 nm ($\varepsilon_{red} = 2100\,M^{-1}cm^{-1}$).

To compare the scavenging efficiency of e_{CB}^-, the amounts of POMs adsorbed on the surface of the TiO_2 powder (P25, Japan Aerosil) were estimated from the steady-state UV absorption measurements, and the adsorption constants (K_{ad}) for POMs were then determined based on the Langmuir adsorption model.[10a–d,26a] The K_{ad} values were determined to be 5.7, 6.0, and $20\times10^4\,M^{-1}$ for $PW_{12}O_{40}^{3-}$, $SiW_{12}O_{40}^{4-}$, and $H_2W_{12}O_{40}^{6-}$, respectively. The maximum adsorbed quantity per unit mass of TiO_2 was also determined to be 20–30 μmol g^{-1}, which is consistent with that (26.7 μmol g^{-1}) reported by another group.[26a] It seems that the amount of adsorbed POMs on the TiO_2 surface depends on the anion valence of the POMs. The surface of the TiO_2 particles is positively charged in acidic solution, whereas the POMs are negatively charged, thus the adsorption of POMs on the surface of the TiO_2 particles is facilitated by simple Coulombic interactions.[26a,35]

As summarized in Table 1, the concentration of the generated POM^- ($[POM^-]$) increases in the order $SiW_{12}O_{40}^{4-} < PW_{12}O_{40}^{3-} < H_2W_{12}O_{40}^{6-}$, while the K_{ad} values increase in the order $PW_{12}O_{40}^{3-} \leq SiW_{12}O_{40}^{4-} \ll H_2W_{12}O_{40}^{6-}$. In particular, a relatively high POM^- concentration was observed for $PW_{12}O_{40}^{3-}$ compared with that for $SiW_{12}O_{40}^{4-}$, although the K_{ad} values for $PW_{12}O_{40}^{3-}$ and $SiW_{12}O_{40}^{4-}$ are almost identical. Therefore, we consider that the efficiency of the e^- scavenging process can be mainly explained in terms of the E_{red} values of the POMs.

One-electron oxidation of aromatic sulfides: In the presence of (methylthio)toluene (MTT; 0.5 mM), a new absorption band with a peak at 550 nm is clearly observed at >5 μs, as shown in Figure 4A. The differential spectrum (open diamonds in Figure 4A), which is obtained by subtracting the transient absorption spectrum for the $TiO_2/PW_{12}O_{40}^{3-}$ from that for $TiO_2/PW_{12}O_{40}^{3-}$/MTT at 20 μs, is quite consistent with that (broken line) of $MTT^{\bullet+}$ obtained from pulse radiolysis measurements. As shown in Figures 4B and 4C, the obtained kinetic traces also strongly suggest that $MTT^{\bullet+}$ is generated in the microsecond time regime (traces c and d).

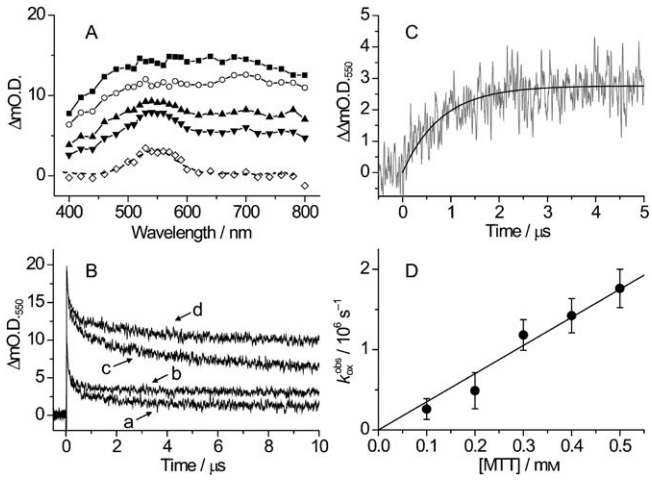

Figure 4. A) Transient absorption spectra observed at 0.1 (solid squares), 0.5 (open circles), 5 (solid triangles), and 20 μs (open inverted triangles) after the laser flash during the 355-nm laser photolysis of argon-saturated $TiO_2/PW_{12}O_{40}^{3-}$ colloidal solutions in the presence of MTT (0.5 mM). The open diamonds in (A) indicate the differential transient absorption spectrum obtained by subtracting the transient absorption spectrum for $TiO_2/PW_{12}O_{40}^{3-}$ from that for $TiO_2/PW_{12}O_{40}^{3-}$/MTT at 20 μs. The broken line indicates the transient absorption spectrum of $MTT^{\bullet+}$ generated by the pulse-radiolysis technique. B) Time traces observed at 550 nm during the 355-nm laser flash photolysis of argon-saturated TiO_2 colloidal solution in the absence (a) and presence (b) of MTT (0.5 mM), and of the $TiO_2/PW_{12}O_{40}^{3-}$ colloidal solution in the absence (c) and presence (d) of MTT (0.5 mM). (C) The differential time trace obtained from trace (d) minus trace (c) in (B). The solid line indicates the single exponential fit. D) Dependence of the observed one-electron oxidation reaction rates (k_{ox}^{obs}) for an argon-saturated $TiO_2/PW_{12}O_{40}^{3-}$/MTT colloidal solution on the MTT concentration.

A slight increase in the signal intensity was observed for bare TiO_2 due to the generation of $MTT^{\bullet+}$ (traces a and b).

The resulting $MTT^{\bullet+}$ concentration for $TiO_2/PW_{12}O_{40}^{3-}$ at [MTT] = 0.5 mM was calculated to be $(4.3\pm0.4)\times10^{-7}$ M using an $\varepsilon_{550}{}^{\bullet+}$ value of 6700 $M^{-1}cm^{-1}$.[36] This value is almost twice that of bare TiO_2. This result suggests that $PW_{12}O_{40}^{3-}$ can assist in the generation of the photogenerated oxidizing species because of its effective electron scavenging from the CB of TiO_2.

The fact that $MTT^{\bullet+}$ is not generated within the laser duration of 5 ns indicates that MTT is not directly oxidized by the valence band h^+ ($h_{VB}{}^+$) at the present concentrations. As is well-known, $h_{VB}{}^+$ is promptly scavenged by chemisorbed molecules that chelate the Ti atom at the surface.[10,37] This reaction is very rapid and competes with the charge recombination and trapping of $h_{VB}{}^+$ by other surface defects. In fact, we have observed the formation of $MTT^{\bullet+}$ within the laser duration of 5 ns during the 355-nm laser photolysis of TiO_2 powder at a higher concentration of MTT (10 mM) in acetonitrile.[10a,c] In addition, no formation of $MTT^{\bullet+}$ in the microsecond time regime was observed in the presence of hole scavengers, such as 2-propanol and *tert*-butyl alcohol. Based on these experimental results, one can consider that the oxidizing species is one or both of $h_{tr}{}^+$, $OH_s^{\bullet}$, and a free $OH^{\bullet}$ ($OH_f^{\bullet}$).

To clarify the one-electron oxidation mechanism, we estimated the rate constant (k_{ox}) from the relationship between the observed formation rates of $MTT^{\bullet+}$ ($k_{ox}{}^{obs}$) and the MTT concentrations, as shown in Figure 4D.

The determined k_{ox} value of $(3.5\pm0.3)\times10^9\,M^{-1}s^{-1}$ is significantly smaller than that of MTT ($(8\pm2)\times10^9\,M^{-1}s^{-1}$) by $OH_f^{\bullet}$ in acidic water (pH 1), which was determined from the pulse radiolysis measurements, thereby suggesting that $OH_f^{\bullet}$ is not the oxidizing species in the present system. As previously reported, the energy of $h_{tr}{}^+$ is in the range of $+1.6\,V \le \equiv TiO^{\bullet-}, H^+/\equiv TiOH \le +1.7\,V$ versus NHE,[38] which is sufficient for the one-electron oxidation of MTT. On the other hand, some groups have reported that $OH_s^{\bullet}$ has a peak at about 350 nm using a pulse-radiolysis technique.[16,17] The redox potential of +1.5 V versus NHE for $OH_s^{\bullet}$, which is insufficient for the one-electron oxidation of MTT, was determined from the oxidation kinetics of SCN^-.[16] However, it is considered that the redox potential of $OH_s^{\bullet}$ is slightly higher than this value because the one-electron oxidation of aromatic sulfides such MTPM (+1.59 V versus NHE) and 2-phenythioethanol (+1.67 V vs. NHE) has been reported.[17]

Unfortunately, $OH_s^{\bullet}$ is kinetically indistinguishable from $h_{tr}{}^+$ in the present aqueous systems. Therefore, $MTT^{\bullet+}$ was generated by the one-electron oxidation with $h_{tr}{}^+$ or $OH_s^{\bullet}$, as given by Equations (4) and (5).

$$h_{VB}{}^+ + H_2O \text{ or } OH^- \rightarrow h_{tr}{}^+ \text{ or } OH_s^{\bullet} \ (+H^+) \quad (4)$$

$$h_{tr}{}^+ \text{ or } OH_s^{\bullet} + MTT \rightarrow MTT^{\bullet+} \quad (5)$$

These results present strong evidence for the indirect one-electron oxidation of organic compounds during the TiO_2 photocatalytic reactions. The relatively small k_{ox} value is mainly due to the steric hindrance of the TiO_2 surface, that is, the decrease in the spatial freedom of the reaction and/or the lower oxidation potentials of $h_{tr}{}^+$ and $OH_s^{\bullet}$ compared with that (+2.72 V versus NHE) of $OH_f^{\bullet}$ in an aqueous acidic solution.[39]

We also observed the transient absorption spectra during the 355-nm laser photolysis of argon-saturated $TiO_2/PW_{12}O_{40}^{3-}$ colloidal solutions in the presence of 4-(methylthio)phenyl methanol (MTPM; 0.5 mM) and 4-(methylthio)-phenylacetic acid (MTPA; 0.5 mM), as shown in Figures 5A and 5C, respectively. For both systems, and particularly in the case of MTPA, transient absorption bands with a peak at about 550 nm, which are assigned to $MTPM^{\bullet+}$ and $MTPA^{\bullet+}$,[40,41] were observed immediately after a laser flash, clearly suggesting that the one-electron oxidation of the substrate (S) occurs by $h_{VB}{}^+$ on the surface of TiO_2 within the laser pulse duration of 5 ns, as given by Equation (6)

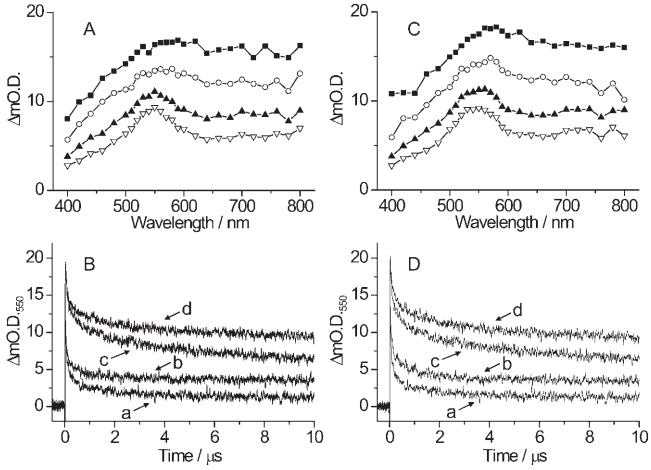

Figure 5. Transient absorption spectra observed at 0.1 (solid squares), 0.5 (open circles), 5 (solid triangles), and 20 μs (open inverted triangles) after the laser flash during the 355-nm laser photolysis of argon-saturated $TiO_2/PW_{12}O_{40}^{3-}$ colloidal solutions in the presence of MTPM (0.5 mM) (A) and MTPA (0.5 mM) (C). Time traces observed for MTPM (B) and MTPA (D) at 550 nm during the 355-nm laser flash photolysis of an argon-saturated TiO_2 colloidal solution in the absence (a) and presence (b) of substrate (0.5 mM), and of the $TiO_2/PW_{12}O_{40}^{3-}$ colloidal solution in the absence (c) and presence (d) of substrate (0.5 mM).

$$h_{VB}{}^+ + S \rightarrow S^{\bullet+} \quad (6)$$

It is noteworthy that the ratio of the maximum concentration of $S^{\bullet+}$ ($[S^{\bullet+}]_{max}$) for $TiO_2/PW_{12}O_{40}^{3-}$ to $[S^{\bullet+}]_{max}$ for TiO_2 increases in the order MTPA < MTPM < MTT, as summarized in Table 2. The present results indicate that the one-electron oxidation processes depend on the properties of the organic compounds, for example the oxidation potential (E_{ox}) and the adsorption ability. The excess adsorption of S on the TiO_2 surface would inhibit this enhancement effect due to competitive adsorption processes between S and POMs.

Table 2. The maximum concentration of $S^{\bullet+}$ ($[S^{\bullet+}]_{max}$) generated during the 355-nm laser flash photolysis of argon-saturated TiO_2 and $TiO_2/PW_{12}O_{40}^{3-}$ colloidal solutions in the presence of substrates (S).

Substrate[a]	$[S^{\bullet+}]_{max}$[b] [μM]		E_{ox}[c]	K_{ad}[c]
	TiO_2	$TiO_2/PW_{12}O_{40}^{3-}$	[V vs. NHE]	[M^{-1}]
MTT	0.26 ± 0.03	0.43 ± 0.04 (1.7)[d]	1.57	20 ± 5
MTPM	0.38 ± 0.04	0.48 ± 0.05 (1.3)[d]	1.59	60 ± 10
MTPA	0.43 ± 0.04	0.49 ± 0.04 (1.1)[d]	1.67	11000 ± 4000

[a] At [S] of 0.5 mM. [b] Calculated from $\varepsilon^{\bullet+}$ and ΔO.D. [c] From reference [10c]. [d] Ratio of $[S^{\bullet+}]_{max}$ for $TiO_2/PW_{12}O_{40}^{3-}$ to $[S^{\bullet+}]_{max}$ for TiO_2.

Electron injection from POM^{-}* into the conduction band of TiO_2: Next, we confirmed the possibility of electron transfer from POM^- in the excited state (POM^{-*}) using a two-color two-laser flash-photolysis technique.

Figure 6A shows the transient absorption spectra observed after a second, 532-nm laser flash (100 mJ per pulse, 5 ns FWHM) following the first 355 nm laser flash with a

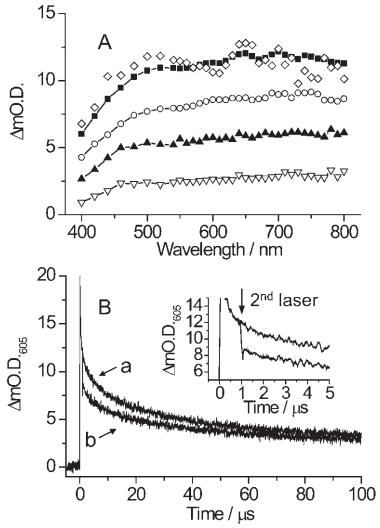

Figure 6. A) Transient absorption spectra obtained at 0.1 μs (solid squares) before and 0.2 (open circles), 4 (solid triangles), and 20 μs (open inverted triangles) after a second, 532-nm laser flash (100 mJ per pulse, 5 ns FWHM) following the first, 355-nm laser flash with a delay time of 1 μs during the two-color two-laser flash photolysis of an argon-saturated $TiO_2/PW_{12}O_{40}^{3-}$ colloidal solution. The open diamonds indicate the normalized differential transient absorption spectrum obtained from open circles (after second, 532-nm laser flash) minus solid squares (before second, 532-nm laser flash). B) Time traces observed at 605 nm during one-laser (a) and two-color two-laser (b) flash photolysis of the argon-saturated $TiO_2/PW_{12}O_{40}^{3-}$ colloidal solution.

delay time of 1 μs during the two-color two-laser flash photolysis of an argon-saturated $TiO_2/PW_{12}O_{40}^{3-}$ colloidal solution at room temperature. Bleaching of the absorption band was clearly observed immediately after the second laser flash, as shown in Figure 6B (trace b).

On the other hand, no detectable bleaching was observed for the bare TiO_2, which indicates that the observed bleaching is due to electron injection from $PW_{12}O_{40}^{4-*}$ into the CB of TiO_2. The spectrum that appeared immediately after the 532-nm laser flash (open circles in Figure 6A) is almost identical to that before the 532-nm laser flash (solid squares), which is mainly assigned to h_{tr}^+ and $PW_{12}O_{40}^{4-}$. A similar tendency was observed for the other POMs. The normalized differential spectrum (open diamonds) is juxtaposed on the spectrum observed before the 532-nm laser flash, suggesting that most of the injected e^- recombine with h_{tr}^+ in TiO_2 within the laser duration of 5 ns, as given by Eqsuations (7) and (8).

$$POM^{-*} + TiO_2 \rightarrow POM + e_{CB}^- \quad (7)$$

$$e_{CB}^-(e_{tr}^-) + h_{tr}^+ \rightarrow TiO_2 + h\nu \quad (8)$$

From the ε value of $2000\ M^{-1}cm^{-1}$ at 751 nm for $PW_{12}O_{40}^{4-}$,[32] one can estimate the decrease in concentration of the injected e^- due to the charge recombination with h_{tr}^+ as $(1.6\pm0.2)\times10^{-6}$ M.

Such photostimulated charge recombination has already been reported by Shkrob et al.[7a] They found that 532- or 1064-nm laser photoexcitation of e_{tr}^- generated during the 355-nm laser flash photolysis of TiO_2 nanoparticles causes rapid photobleaching of the absorption bands in the visible and near-IR regions. This photobleaching occurs within the duration of the laser pulse (6 ns) and is caused by photoinduced e^- de-trapping followed by recombination of the resulting free e_{CB}^- and h_{tr}^+.

It should also be noted that a deceleration of the decay process was observed, as shown in Figure 6B. This deceleration indicates a decrease in concentration of h_{tr}^+, which is due to the photostimulated charge-recombination process between injected e^- and h_{tr}^+.

Electron storage in the $TiO_2/PW_{12}O_{40}^{3-}/MV^{2+}$ ternary system: As discussed above, it is expected that irradiation of $TiO_2/PW_{12}O_{40}^{3-}$ with UV or visible-light should not be effective for the photocatalytic reaction because of the fast charge-recombination between e_{CB}^- (e_{tr}^-) and h_{tr}^+ via $PW_{12}O_{40}^{4-*}$. To maintain the electron trapped in $PW_{12}O_{40}^{4-}$ adsorbed on the TiO_2 surface, we used methyl viologen (MV^{2+}) as an electron mediator.

As shown in Figure 7A, the transient absorption spectra obtained during the two-color two-laser flash photolysis of $TiO_2/PW_{12}O_{40}^{3-}$ in the presence of MV^{2+} (10 mM) are quite similar to those obtained during the 355-nm laser flash photolysis of $TiO_2/PW_{12}O_{40}^{3-}$ (Figure 2B). The extent of bleaching also decreases with increasing MV^{2+} concentration, as shown in Figure 7B. In acidic solution, MV^{2+} cannot be adsorbed on the surface of the TiO_2 particles because of the electrically positive surface due to the adsorption of H^+.[31] In addition, the E_{red} value of MV^{2+} (−0.45 V versus NHE)[42] is more negative than that of e_{CB}^- (-0.19 V vs. NHE),[34] which suggests that direct electron transfer from e_{CB}^- to MV^{2+} is quite difficult. The fact that no recovery was observed in the presence of neutral electron acceptors such as chloroacetonitrile (0.16 M; −0.52 V versus NHE)[43] suggests that complex formation between $PW_{12}O_{40}^{3-}$ and

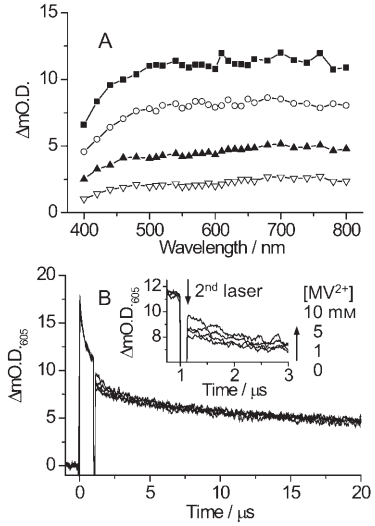

Figure 7. A) Transient absorption spectra obtained at 0.1 μs (solid squares) before and 0.3 (open circles), 4 (solid triangles), and 30 μs (open inverted triangles) after a second, 532-nm laser flash (100 mJ per pulse, 5 ns FWHM) following the first, 355-nm laser flash with a delay time of 1 μs during the two-color two-laser flash photolysis of an argon-saturated $TiO_2/PW_{12}O_{40}^{3-}$ colloidal solution in the presence of MV^{2+} (10 mM). B) Time traces observed at 605 nm during the two-color two-laser flash photolysis of the argon-saturated $TiO_2/PW_{12}O_{40}^{3-}$ colloidal solution in the absence and presence of MV^{2+} (1–10 mM).

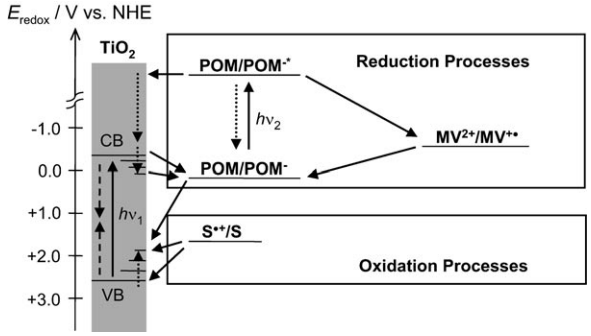

Figure 8. Energy diagram for the TiO_2/POM photocatalytic redox processes. Dotted and broken arrows represent the deactivation and charge-recombination processes between e_{CB}^- or e_{tr}^- and h_{VB}^+ or h_{tr}^+, respectively.

MV^{2+} occurs. Kochi and co-workers have reported the formation of charge-transfer complexes in the solid state between POM and aromatic compounds that have a cationic pyridinium or trialkylammonium substituent.[44] Thus, we considered that $MV^{\bullet+}$ is generated by electron transfer from $PW_{12}O_{40}^{4-*}$ to MV^{2+}, where the Coulombic interaction between the anionic $PW_{12}O_{40}^{4-}$ and cationic MV^{2+} would support the complex formation, as given by Equation (9).

$$POM^{\bullet-}/MV^{2+} \rightarrow POM/MV^{\bullet+} \quad (9)$$

In addition, the E_{red} value of MV^{2+} is much more negative than that of $PW_{12}O_{40}^{3-}$ (+0.218 V vs. NHE),[23b] thus indicating that the cascade electron transfer from $MV^{\bullet+}$ to $PW_{12}O_{40}^{3-}$ is energetically possible. Therefore, no transient absorption band with a peak at about 600 nm,[31] which is attributable to $MV^{\bullet+}$, is observed after the second laser pulse.

Mechanisms of the POM-mediated TiO_2 photocatalytic redox reactions: Figure 8 summarizes the energy diagram for the TiO_2/POM photocatalytic redox processes. For the one-electron oxidation processes, the efficiency of the one-electron oxidation of substrates by $OH_s^{\bullet}$ is significantly enhanced due to electron transfer from the CB of TiO_2 to POM. However, the excess adsorption of substrates on the TiO_2 surface inhibits this enhancement effect due to competitive adsorption processes between the substrates and POM.

For the one-electron reduction processes, POM^- is generated from a one-electron reduction by e_{CB}^- in TiO_2 and subsequently absorbs visible light to form POM^{-*}. The generated POM^{-*} then injects electrons into the CB of TiO_2 within the laser duration. In the presence of a cationic electron acceptor such as MV^{2+}, however, electron transfer from POM^{-*} to MV^{2+} is observed. Finally, a cascade electron transfer from $MV^{\bullet+}$ to POM occurs to give POM^-. Our observations clearly suggest the formation of a pre-associated complex or a pre-associated equilibrium of POM with the electron acceptor in aqueous solution.

Conclusion

In conclusion, we have successfully investigated the one-electron oxidation and reduction processes of several compounds during POM-mediated TiO_2 photocatalytic reactions using a two-color two-laser flash-photolysis technique. It should be noted that both processes were examined using the same system. For the one-electron oxidation processes, the efficiency of the one-electron oxidation of MTT by h_{tr}^+ or $OH_s^{\bullet}$ is significantly enhanced due to electron transfer from the CB of TiO_2 to $PW_{12}O_{40}^{3-}$. According to the determined K_{ad} values between POMs and TiO_2, it seems that the efficiency of the electron transfer from the CB of TiO_2 to the POM increases in the order $H_2W_{12}O_{40}^{6-} < SiW_{12}O_{40}^{4-} < PW_{12}O_{40}^{3-}$, that is, it depends on the E_{red} values of the POMs. For the one-electron reduction processes, we observed electron injection from $PW_{12}O_{40}^{4-*}$ to the CB of TiO_2, and achieved storage of the electrons in the $TiO_2/PW_{12}O_{40}^{3-}/MV^{2+}$ ternary system using a two-color two-laser irradiation. The present results will lead to further application of TiO_2/POM photocatalysts and demonstrate that the two-color two-laser flash-photolysis technique is a powerful tool for the investigation of interfacial electron transfer at the heterogeneous surfaces of nanocomposite materials.

Experimental Section

Materials: Colloidal aqueous solutions of TiO_2 were prepared by the controlled hydrolysis of $TiCl_4$ at 2 °C. In a typical preparation, 7.58 g of fresh

$TiCl_4$ (Wako) was slowly added dropwise over 1 h to 1 L of Milli-Q water (2–4 °C) with vigorous stirring. The 0.3 L TiO_2 colloidal solutions were subsequently dialyzed at 4 °C (Visking tube presoaked for one week in approximately 2.5 L of Milli-Q water, which was replaced several times per day), resulting in a pH of 1.0 for the colloidal solution ($[Cl^-] = 4.5 \times 10^{-6}$ M). Dynamic light scattering (Horiba, LB-550) indicated that the mean particle size of the material was 16 nm. $H_3PW_{12}O_{40}$ (Aldrich), $Na_4SiW_{12}O_{40}$ (Nippon Inorganic Colour & Chemical), and $(NH_4)_6H_2W_{12}O_{40}$ (Aldrich) were used without further purification as the ion source. Methyl viologen dichloride hydrate (MV^{2+}) (Tokyo Kasei) was used as an electron acceptor without further purification. 4-(Methylthio)toluene (MTT; Tokyo Kasei) was used without further purification. 4-(Methylthio)phenyl methanol (MTPM) (Aldrich) was purified by vacuum sublimation before use. 4-(Methylthio)phenylacetic acid (MTPA) was recrystallized from ethanol. Chloroacetonitrile (Tokyo Kasei) was used as an electron acceptor without further purification. 2-Propanol (Wako) and *tert*-butyl alcohol (Nacalai Tesque) were used as hole scavengers without further purification.

Adsorption of the POMs on the TiO_2 surface: To estimate the amount of adsorbed POMs on the TiO_2 surface, aqueous solutions (pH 1) of POMs (0.05–0.5 mM) and the TiO_2 powder (P25, Japan Aerosil) (5 g L^{-1}) were sonicated for 10 min, and the TiO_2 particles in suspension were then completely removed by centrifugation (10000 rpm, 10 min) in a high-speed microcentrifuge (Hitachi, himac CF16RX) at 22 °C for the UV absorption measurements. All procedures for the sample preparation were performed with shielding from UV light. The steady-state UV absorption spectra were measured with a UV-Vis–NIR spectrophotometer (Shimadzu, UV-3100) at room temperature.

One-laser flash photolysis: The one-laser flash-photolysis experiments were performed by using the third harmonic generation (355 nm, 5 ns full width at half-maximum) from a Q-switched Nd^{3+}:YAG laser (Continuum, Surelite II-10) for the excitation operated with temporal control by a delay generator (Stanford Research Systems, DG535). The analyzing light from a 450-W Xe arc lamp (Ushio, UXL-451-0) was collected by a focusing lens and directed through a grating monochromator (Nikon, G250) onto a silicon avalanche photodiode detector (Hamamatsu Photonics, S5343). The analyzing lamp, sample, monochromator, and photodiode detector all lie on the same axis, with the excitation beam incident at 90° to the axis. The transient signals were recorded with a digitizer (Tektronix, TDS 580D). Suitable filters were employed to avoid stray light and pyrolysis of the sample by the probe light. The samples were contained in a transparent rectangular quartz cell ($10 \times 10 \times 40$ mm^3). All measurements were carried out at room temperature. The irradiation energy was measured using a power meter.

Two-color two-laser flash photolysis: The two-color two-laser flash-photolysis experiments were carried out using the third harmonic oscillation (355 nm) of an Nd^{3+}:YAG laser (Quantel, Brilliant; 5 ns fwhm) as the first laser and the 532-nm flash from a Q-switched Nd^{3+}:YAG laser (Continuum, Surelite II-10) as the second laser. The delay time of the two laser flashes was adjusted to 1 μs by the delay generators (Stanford Research Systems, model DG 535). The two laser beams were adjusted so as to overlap at the sample.

Pulse radiolysis: Pulse-radiolysis experiments were performed using an electron pulse (28 MeV, 8 ns, 0.87 kGy per pulse) from a linear accelerator at Osaka University. All experiments were performed with aqueous acidic solutions (pH 1) that had been saturated with purified N_2O gas for a minimum of 20 min by a capillary technique. Saturation of the solution with N_2O was done to quantitatively convert all solvated electrons into $OH^{\bullet}$ in the radiolysis experiments. The kinetic measurements were performed with a nanosecond photoreaction analyzer system (Unisoku, TSP-1000). The monitor light was obtained from a pulsed 450-W Xe arc lamp (Ushio, UXL-451–0), which was connected to a large-current, pulsed-power supply that was synchronized with the electron pulse. The monitor light was passed through an iris with a diameter of 0.2 cm and sent into the sample solution at a perpendicular intersection to the electron pulse. The monitor light passing through the sample was focused on the entrance slit of a monochromator (Unisoku, MD200) and detected with a photomultiplier (Hamamatsu Photonics, R2949). The transient absorption spectra were measured using a photodiode array (Hamamatsu Photonics, S3904-1024F) with a gated image intensifier (Hamamatsu Photonics, C2925-01) as detector.

Acknowledgments

The authors thank the staff of the Radiation Laboratory of the Institute of Scientific and Industrial Research at Osaka University for running the pulse-radiolysis experiments. The authors are grateful to Dr. J. Ichihara (Osaka University) for supplying some of the POMs. This work was partly supported by a Grant-in-Aid for Scientific Research (Project 17105005, Priority Area (417), 21 st Century COE Research, and others) from the Ministry of Education, Culture, Sports, Science and Technology (MEXT) of the Japanese Government.

[1] See, for example: a) D. M. Adams, L. Brus, C. E. D. Chidsey, S. Creager, C. Creutz, C. R. Kagan, P. V. Kamat, M. Lieberman, S. Lindsay, R. A. Marcus, R. M. Metzger, M. E. Michel-Beyerle, J. R. Miller, M. D. Newton, D. R. Rolison, O. Sankey, K. S. Schanze, J. Yardley, X. J. Zhu, *J. Phys. Chem. B* **2003**, *107*, 6668–6697; b) E. Katz, I. Willner, *Angew. Chem.* **2004**, *116*, 6166–6235; *Angew. Chem. Int. Ed.* **2004**, *43*, 6042–6108; c) T. Paunesku, T. Rajh, G. Wiederrecht, J. Maser, S. Vogt, N. Stojićević, M. Protić, B. Lai, J. Oryhon, M. Thurnauer, G. Woloschak, *Nat. Mater.* **2003**, *2*, 343–346.

[2] See, for example: a) M. A. Fox, M. T. Dulay, *Chem. Rev.* **1993**, *93*, 341–357; b) M. R. Hoffmann, S. T. Martin, W. Choi, D. W. Bahnemann, *Chem. Rev.* **1995**, *95*, 69–96; c) A. Hagfeldt, M. Grätzel, *Chem. Rev.* **1995**, *95*, 49–68; d) A. Mills, S. L. Hunte, *J. Photochem. Photobiol. A* **1997**, *108*, 1–35; e) A. Fujishima, T. N. Rao, D. A. Tryk, *J. Photochem. Photobiol. C* **2000**, *1*, 1–21; f) M. Anpo, *Bull. Chem. Soc. Jpn.* **2004**, *77*, 1427–1442.

[3] a) G. Rothenberger, J. Moser, M. Grätzel, N. Serpone, D. K. Sharma, *J. Am. Chem. Soc.* **1985**, *107*, 8054–8059; b) N. Serpone, D. Lawless, R. Khairutdinov, E. Pelizzetti, *J. Phys. Chem.* **1995**, *99*, 16655–16661.

[4] D. Bahnemann, A. Henglein, J. Lilie, L. Spanhel, *J. Phys. Chem.* **1984**, *88*, 709–711.

[5] D. W. Bahnemann, M. Hilgendorff, R. Memming, *J. Phys. Chem. B* **1997**, *101*, 4265–4275.

[6] a) D. P. Colombo, Jr., R. M. Bowman, *J. Phys. Chem.* **1995**, *99*, 11752–11756; b) D. P. Colombo, Jr., R. M. Bowman, *J. Phys. Chem.* **1996**, *100*, 18445–18449.

[7] a) I. A. Shkrob, M. C. Sauer Jr., *J. Phys. Chem. B* **2004**, *108*, 12497–12511; b) I. A. Shkrob, M. C. Sauer, Jr., D. Gosztola, *J. Phys. Chem. B* **2004**, *108*, 12512–12517.

[8] a) A. Furube, T. Asahi, H. Masuhara, H. Yamashita, M. Anpo, *J. Phys. Chem. B* **1999**, *103*, 3120–3127; b) A. Furube, T. Asahi, H. Masuhara, H. Yamashita, M. Anpo, *Res. Chem. Intermed.* **2001**, *27*, 177–187.

[9] T. Yoshihara, R. Katoh, A. Furube, Y. Tamaki, M. Murai, K. Hara, S. Murata, H. Arakawa, M. Tachiya, *J. Phys. Chem. B* **2004**, *108*, 3817–3823.

[10] a) T. Tachikawa, S. Tojo, M. Fujitsuka, T. Majima, *Chem. Phys. Lett.* **2004**, *382*, 618–625; b) T. Tachikawa, S. Tojo, M. Fujitsuka, T. Majima, *Langmuir* **2004**, *20*, 2753–2759; c) T. Tachikawa, S. Tojo, M. Fujitsuka, T. Majima, *J. Phys. Chem. B* **2004**, *108*, 5859–5866; d) T. Tachikawa, A. Yoshida, S. Tojo, A. Sugimoto, M. Fujitsuka, T. Majima, *Chem. Eur. J.* **2004**, *10*, 5345–5353; e) T. Tachikawa, S. Tojo, M. Fujitsuka, T. Majima, *J. Phys. Chem. B* **2004**, *108*, 11054–11061; f) T. Tachikawa, S. Tojo, K. Kawai, M. Endo, M. Fujitsuka, T. Ohno, K. Nishijima, Z. Miyamoto, T. Majima, *J. Phys. Chem. B* **2004**, *108*, 19299–19306.

[11] a) K. Ishibashi, Y. Nosaka, K. Hashimoto, A. Fujishima, *J. Phys. Chem. B* **1998**, *102*, 2117–2120; b) K. Ishibashi, A. Fujishima, T. Watanabe, K. Hashimoto, *J. Phys. Chem. B* **2000**, *104*, 4934–4938;

c) Y. Nosaka, M. Nakamura, T. Hirakawa, *Phys. Chem. Chem. Phys.* **2002**, *4*, 1088–1092.

[12] a) T. Tatsuma, S. Tachibana, A. Fujishima, *J. Phys. Chem. B* **2001**, *105*, 6987–6992; b) T. Tatsuma, W. Kubo, A. Fujishima, *Langmuir* **2002**, *18*, 9632–9634; c) W. Kubo, T. Tatsuma, A. Fujishima, H. Kobayashi, *J. Phys. Chem. B* **2004**, *108*, 3005–3009.

[13] a) R. F. Howe, M. Grätzel, *J. Phys. Chem.* **1987**, *91*, 3906–3909; b) O. I. Micic, Y. Zhang, K. R. Cromack, A. D. Trifunac, M. C. Thurnauer, *J. Phys. Chem.* **1993**, *97*, 7277–7283; c) M. A. J. Grela, M. E. Coronel, A. J. Colussi, *J. Phys. Chem.* **1996**, *100*, 16940–16946; d) P. F. Schwarz, N. J. Turro, S. H. Bossmann, A. M. Braun, A.-M. A. Abdel Wahab, H. Dürr, *J. Phys. Chem. B* **1997**, *101*, 7127–7134; e) Y. Nakaoka, Y. Nosaka, *J. Photochem. Photobiol. A* **1997**, *110*, 299–305.

[14] a) Y. Nosaka, M. Kishimoto, J. Nishio, *J. Phys. Chem. B* **1998**, *102*, 10279–10283; b) T. Hirakawa, Y. Nosaka, *Langmuir* **2002**, *18*, 3247–3254.

[15] M. W. Petelson, J. A. Tumer, A. J. Nozik, *J. Phys. Chem.* **1991**, *95*, 221–225.

[16] D. Lawless, N. Serpone, D. Meisel, *J. Phys. Chem.* **1991**, *95*, 5166–5170.

[17] a) S. Tojo, T. Tachikawa, M. Fujitsuka, T. Majima, *Chem. Phys. Lett.* **2004**, *384*, 312–316; b) S. Tojo, T. Tachikawa, M. Fujitsuka, T. Majima, *Phys. Chem. Chem. Phys.* **2004**, *6*, 960–964.

[18] a) T. L. Villarreal, R. Gómez, M. Neumann-Spallart, N. Alonso-Vante, P. Salvador, *J. Phys. Chem. B* **2004**, *108*, 15172–15181; b) T. L. Villarreal, R. Gómez, M. González, P. Salvador, *J. Phys. Chem. B* **2004**, *108*, 20278–20290.

[19] a) R. Nakamura, A. Imanishi, K. Murakoshi, Y. Nakato, *J. Am. Chem. Soc.* **2003**, *125*, 7443–7450; b) R. Nakamura, Y. Nakato, *J. Am. Chem. Soc.* **2004**, *126*, 1290–1298.

[20] a) P. C. Lee, D. Meisel, *J. Catal.* **1981**, *70*, 160–167; b) C. M. Wang, A. Heller, H. Gerischer, *J. Am. Chem. Soc.* **1992**, *114*, 5230–5234.

[21] a) W. Choi, A. Termin, M. R. Hoffmann, *J. Phys. Chem.* **1994**, *98*, 13669–13679; b) A. Di Paola, G. Marcì, L. Palmisano, M. Schiavello, K. Uosaki, S. Ikeda, B. Ohtani, *J. Phys. Chem. B* **2002**, *106*, 637–645.

[22] a) M. Takeuchi, K. Tsujimaru, K. Sakamoto, M. Matsuoka, H. Yamashita, M. Anpo, *Res. Chem. Intermed.* **2003**, *29*, 619–629; b) V. Subramanian, E. E. Wolf, P. V. Kamat, *Langmuir* **2003**, *19*, 469–474.

[23] See, for example: a) C. L. Hill, C. M. Prosser-McCartha, *Coord. Chem. Rev.* **1995**, *143*, 407–455; b) I. A. Weinstock, *Chem. Rev.* **1998**, *98*, 113–170; c) T. Yamase, *Chem. Rev.* **1998**, *98*, 307–325; d) D. E. Katsoulis, *Chem. Rev.* **1998**, *98*, 359–387; e) C. Tanielian, *Coord. Chem. Rev.* **1998**, *178–180*, 1165–1181; f) A. Hiskia, A. Mylonas, E. Papaconstantinou, *Chem. Soc. Rev.* **2001**, *30*, 62–69.

[24] M. Yoon, J. A. Chang, Y. Kim, J. R. Choi, K. Kim, S. J. Lee, *J. Phys. Chem. B* **2001**, *105*, 2539–2545.

[25] a) H. Park, W. Choi, *J. Phys. Chem. B* **2003**, *107*, 3885–3890; b) S. Kim, H. Park, W. Choi, *J. Phys. Chem. B* **2004**, *108*, 6402–6411.

[26] a) C. Chen, P. Lei, H. Ji, W. Ma, J. Zhao, H. Hidaka, N. Serpone, *Environ. Sci. Technol.* **2004**, *38*, 329–337; b) C. Chen, W. Zhao, P. Lei, J. Zhao, N. Serpone, *Chem. Eur. J.* **2004**, *10*, 1956–1965.

[27] R. Ozer, J. Ferry, *Environ. Sci. Technol.* **2001**, *35*, 3242–3246.

[28] a) Y. Yang, Y. Guo, C. Hu, E. Wang, *Appl. Catal. A* **2003**, *252*, 305–314; b) Y. Yang, Y. Guo, C. Hu, C. Jiang, E. Wang, *J. Mater. Chem.* **2003**, *13*, 1686–1694; c) D. Li, C. Gu, C. Guo, C. Hu, *Chem. Phys. Lett.* **2004**, *385*, 55–59; d) Y. Yang, Y. Guo, C. Hu, Y. Wang, E. Wang, *Appl. Catal. A* **2004**, *273*, 201–210.

[29] J. Kiwi, M. Grätzel, *J. Phys. Chem.* **1987**, *91*, 6673–6677.

[30] a) M. Sakamoto, X. Cai, M. Hara, M. Fujitsuka, T. Majima, *J. Am. Chem. Soc.* **2004**, *126*, 9709–9714; b) M. Sakamoto, X. Cai, M. Hara, S. Tojo, M. Fujitsuka, T. Majima, *J. Phys. Chem. A* **2004**, *108*, 10941–10948.

[31] T. Tachikawa, S. Tojo, M. Fujitsuka, T. Majima, *Langmuir* **2004**, *20*, 9441–9444.

[32] a) The molar absorbance coefficients (ε) of $PW_{12}O_{40}^{4-}$, $SiW_{12}O_{40}^{5-}$, and $H_2W_{12}O_{40}^{7-}$ are 2000 $M^{-1}cm^{-1}$ at 751 nm, 2100 $M^{-1}cm^{-1}$ at 729 nm, and 2100 $M^{-1}cm^{-1}$ at 689 nm, respectively.[32b] The blue color of POM^- is attributed to the intervalence charge-transfer of electrons between W^{6+} and W^{5+}; b) G. M. Varga, Jr., E. Papaconstantinou, M. T. Pope, *Inorg. Chem.* **1970**, *9*, 662–667.

[33] a) It was initially attributed to a very strong antiferromagnetic coupling via a multi-route superexchange mechanism,[33b,c] but more recently it has been theoretically shown that the combination of electron repulsion and electron delocalization can also stabilize the singlet ground state;[33e–g] b) M. Kozik, C. F. Hammer, L. C. W. Baker, *J. Am. Chem. Soc.* **1986**, *108*, 7627–7630; c) N. Casan-Pastor, L. C. W. Baker, *J. Am. Chem. Soc.* **1992**, *114*, 10384–10394; d) S. A. Borshch, B. Bigot, *Chem. Phys. Lett.* **1993**, *212*, 398–402; e) J. J. Borrás-Almenar, J. M. Clemente, E. Coronado, B. S. Tsukerblat, *Chem. Phys.* **1995**, *195*, 1–15; f) J. J. Borrás-Almenar, J. M. Clemente, E. Coronado, B. S. Tsukerblat, *Chem. Phys.* **1995**, *195*, 17–28; g) J. J. Borrás-Almenar, J. M. Clemente, E. Coronado, B. S. Tsukerblat, *Chem. Phys.* **1995**, *195*, 29–47.

[34] D. Duonghong, J. Ramsden, M. Grätzel, *J. Am. Chem. Soc.* **1982**, *104*, 2977–2985.

[35] a) According to solid-state ^{31}P and ^{1}H MAS NMR measurements, the chemical nature of the $PW_{12}O_{40}^{3-}$ adsorbed on powdered TiO_2 has changed.[35b] Analysis of the ^{31}P NMR data indicates that there are at least five types of phosphorus on the TiO_2 surface—a bulk salt phase, two weakly bound intact Keggin unit species, a strongly bound partially fragmented Keggin unit, a strongly bound highly fragmented Keggin unit, and a pure phosphate phase formed by complete fragmentation of the Keggin unit into tungstate and phosphate; b) J. Edward, C. Y. Thiel, B. Benac, J. F. Knifton, *Catal. Lett.* **1998**, *51*, 77–83.

[36] M. Ioele, S. Steenken, E. Baciocchi, *J. Phys. Chem. B* **1997**, *101*, 2979–2987.

[37] T. Rajh, L. X. Chen, K. Lukas, T. Liu, M. C. Thurnauer, D. M. Tiede, *J. Phys. Chem. B* **2002**, *106*, 10543–10552.

[38] O. I. Micic, T. Rajh, M. V. Comor, *Electrochemistry in Colloids and Dispersions* (Eds.: R. A. Mackey, J. Texter), VCH, New York, **1992**, p. 457.

[39] H. A. Schwarz, R. W. Dodson, *J. Phys. Chem.* **1984**, *88*, 3643–3647.

[40] H. Mohan, J. P. Mittal, *J. Phys. Chem. B* **2002**, *106*, 6574–6580.

[41] H. Mohan, J. P. Mittal, *Bull. Chem. Soc. Jpn.* **2001**, *74*, 1649–1659.

[42] P. Wardman, *J. Phys. Chem. Ref. Data* **1989**, *18*, 1637–1755.

[43] C. Costentin, M. Robert, J.-M. Savéant, *J. Am. Chem. Soc.* **1985**, *107*, 10729–10739.

[44] P. Le Maguerès, S. M. Hubig, S. V. Lindeman, P. Veya, J. K. Kochi, *J. Am. Chem. Soc.* **2000**, *122*, 10073–10082.

Received: September 1, 2005
Published online: December 16, 2005

